Tuberculosis 118 (2019) 101852

Contents lists available at ScienceDirect

Tuberculosis

journal homepage: www.elsevier.com/locate/tube

Diagnostics

DARPin based GMR Biosensor for the detection of ESAT-6 Tuberculosis Protein

Shagun Gupta*, Vipan Kakkar

School of Electronics and Communication Engineering, Shri Mata Vaishno Devi University, Katra, 182320, India

ARTICLE INFO

Index Terms:
Tuberculosis
GMR (Giant Magnetoresistance)
ESAT-6
DARPins
ELISA
GNP (Gold Nanoparticles)

ABSTRACT

Tuberculosis (TB), a life threatening communicable disease, is mainly caused by the bacterium named *Mycobacterium tuberculosis* (*MTB*). This high burden infectious threat is the ninth leading killer disease worldwide and also the foremost cause of death from a single infectious agent, even ranking above HIV/AIDS. In this work, a novel magnetic biosensing technique based on giant magneto-resistance (GMR) has been proposed for the on-field detection of Tuberculosis (TB) through assessment of *MTB* specific protein- ESAT-6. This portable highly sensitive diagnostic tool provides the results with a low turnaround time and the achieved limit of detection in the range of pg/ml can be a breakthrough in TB diagnostics. In addition, the use of DARPins (designed ankyrin repeat proteins) leads to high specificity and help in early detection, thus enabling early onset of treatment and thereby reduced mortality. This study compares the results of conventional and GNP-ELISA and it has been shown that the proposed GMR technique is more sensitive. Further, the effect of different sized magnetic nanoparticles on the performance of GMR biosensor is also presented.

1. Introduction

Tuberculosis (TB), a global health challenge mainly caused by the bacterium *Mycobacterium tuberculosis* (*MTB*), is among the top ten leading infectious causes of death as per World Health Organization (WHO) Global TB report 2017 [1]. TB is considered as a major burden-inflicting disease in the world especially in low and middle income countries (LIMC) due to emergence of drug-resistance mutants (DR-TB) which has threatened to jeopardize the universal efforts of controlling this outbreak. One of the major contributors to the increased disease burden is the delayed diagnosis. The delay in diagnosis is largely due to the lack of sensitive diagnostics and heavy reliance on traditional diagnostic methods. In order to overcome this and for the worldwide management of this epidemic, constant global efforts have been made over the last few decades in developing the efficient, cheap and rapid point-of-care TB detection techniques [2] as early stage diagnosis and appropriate treatment on-time are indispensable for controlling TB. In this context, advancements in biosensing technology have the potential of unfolding huge opportunities for fast and accurate TB detection [2].

Magnetic biosensors have gained much interest of researchers in the recent years owing to their capability and high potential of targeting and detecting biomolecules by utilizing the functionalized nanomaterials [3]. Among the various transduction techniques available for designing a biosensor, magnetic biosensors based on magnetoresistive principle can be constructed as a small-sized portable platform that can provide the highly sensitive results at affordable costs. Such sensors are extremely compatible with the standard microfluidics and microfabrication technologies that will help in realizing the real-time on-chip systems for the quantification and detection of various biological analytes like proteins, bacteria, nucleic acids, etc. [4]. This study describes a magnetic biosensor employing the Giant Magnetoresistance (GMR) principle. The GMR effect is based on the electrical resistance of a material that changes with changes in the magnetic field around it and is observed in the sandwich type multilayer geometry. Initially, the geometry is aligned antiparallel with the magnetic field H = 0, and when the external magnetic field is applied, its resistance decreases by more than 50%. Since, the resistance decreases by a very large value, this effect is named as giant magnetoresistance (GMR) [5].

This effect is basically relied on the experimentally proven fact that electron spin can be conserved up to several tens of nanometres. This distance is far greater than typical multilayer thickness, thus in the trilayer (consisting of non-magnetic layer such as copper (Cu) between the two ferromagnetic layers made up of NiCoFe), the electric current flows in two channels. One flow corresponds to the electrons with upward (↑) spin projection and the other corresponds to the electrons with the downward (↓) spin projection. Since the spin is conserved, which

* Corresponding author.
E-mail addresses: 17dec002@smvdu.ac.in (S. Gupta), vipan.kakar@smvdu.ac.in (V. Kakkar).

https://doi.org/10.1016/j.tube.2019.07.003
Received 23 April 2019; Received in revised form 2 July 2019; Accepted 19 July 2019
Available online 20 July 2019
1472-9792/

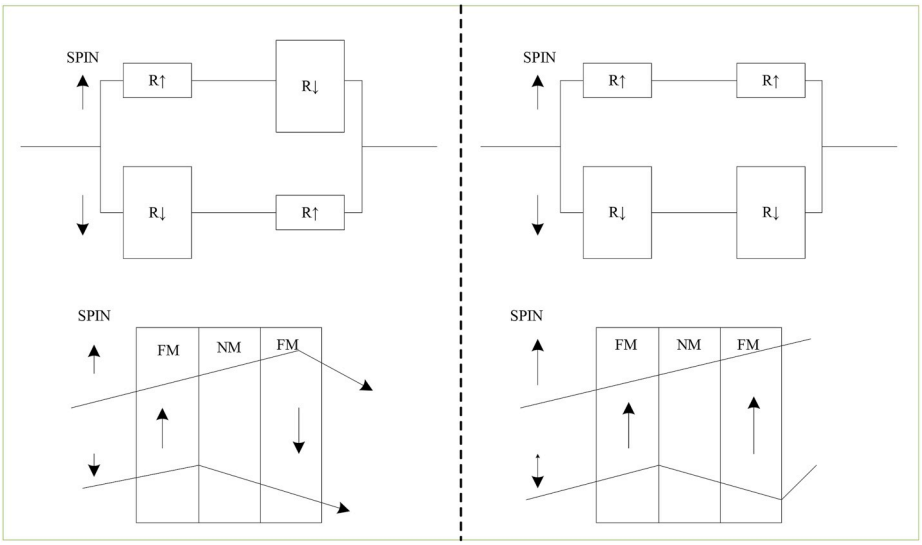

Fig. 1. GMR equivalent Resistor Model [5,7].

means both the upward and downward spin channels are independent, thus these channels can be considered as two wires connected in parallel [6]. Therefore, GMR geometry can be explained by using an equivalent simple resistor model (as shown in Fig. 1). The important observation is that when the electrons, with parallel and antiparallel spin projections to the ferromagnetic (FM) layer magnetization respectively, enter the ferromagnetism; they scattered at varied rates as specified in Fig. 1 [7]. GMR sensors can be designed as a miniaturised, robust platform and further can be integrated with different heterogenic technologies due to the state-of-the-art advancements [8,9]. Also GMR fabrication only involves low temperature processes because of the no-requirement of ionic doping (diffusion and implantation) [10].

It has been visualized that this GMR technology has great application prospects in disease monitor and prevention areas by virtue of its powerful diagnostic capability [11]. GMR-based biosensing system has successfully detected protein biomarkers for various human diseases such as lung cancer, prostate cancer, heart disease, and environmental issues such as mercury pollution [12]. The researchers, in the year 2016–2017, have described the GMR biosensor's capability of detecting influenza A virus with the limit of detection of 1.5×10^2 $TCID_{50}$/mL [13,14]. GMR biosensors can also detect the presence of mercuric ion (Hg^{2+}) with the detection limit of 10 nM in both buffer and natural water [12]. Recently, a GMR sensor array based real-time, multiplexed electrical readout system has been designed in order to detect simultaneously a panel of three different protein biomarkers namely PCSK9, ST2 and PAPP-A for identifying cardiovascular diseases. Early detection of multiple biomarkers for a disease could enable accurate prediction of a disease risk. A detection limit of 40 pg/mL for ST2 antigen, a promising candidate biomarker for cardiovascular disease, has been achieved and the magnitude of up to four orders has been detected when tested for the dynamic ranges of all the three proteins [8]. The detection of S100β biomarker's dose response using GMR sensor has attained a low detection limit of 27 pg/mL [15]. Apart from the detection of protein biomarkers, the biosensors based on GMR technique can also be used to detect the disease specific DNA sequences. This can be done by employing the principle of molecular recognition between specific known DNA sequences immobilized locally at the sensor surface (so-called probe DNA) and the DNA sequences that are to be analyzed (so called analyte DNA) [6]. Furthermore, the GMR based biosensor is expected to be an easy-to-use sensor and able to test multiple diseases in one simple body fluid sample and in one step [11].

In this work, the design of a GMR biosensor is proposed for the detection of Tuberculosis (TB). Identification of a specific target, appearing at the early infection stage, from bacterium *M. tuberculosis* is required for the development of an efficient detection system. ESAT-6 (Early secretory antigenic target) is one among the various antigenic proteins secreted by *M. tuberculosis* at the initial infection stage and is prominent during progression of TB infection, thus considered as the key mediator in mycobacterial virulence [16]. The weight of ESAT-6 is 6 kDa (kilo Daltons), hence it is a small protein that can bind to toll-like receptor-2 (TLR-2) directly and has the capability of inhibiting the downstream transduction of signal transduction. Moreover, culture filtrate protein (CFP-10; another antigenic protein secreted by *M. tuberculosis*) having 10 kDa weight and ESAT-6 together can form a heterodimer, hence leading to virulence [17]. Further, the earlier species specific assumptions about ESAT-6 have been contradicted by Geluk et al. [18]. These researchers have noted the orthologous nature of ESAT-6 among several Mycobacterium pathogenic species. Thus, for the early stage TB diagnosis, developing a platform that can identify ESAT-6 occurrence seems to be a promising strategy.

2. Material and method details

2.1. GMR biosensor chip structure and surface functionalization

The proposed biosensor consists of two wires sandwiched between a silicon substrate and an insulating adsorptive layer such as SiO_2. One of these wires is a conductor (for constant current) and other one is GMR. The topside of the insulator is coated with a layer of immobilized analyte, in this case DARPin (designed ankyrin repeat protein), which is designed to specifically attract the MTB secretory antigens- Early secreted antigenic target-6 (ESAT-6).

For the practical implementation, DARPins are needed to be constructed. The DARPin library construction procedure involves double strand DNA synthesis using the NNK/NNS method, also introducing variations in desired number of positions (maximum, n = 7). The constructed double stranded DNA would be ligated and transformed. The library thus generated has diversity in the range of 10^8-10^{12}. These variants are then screened using the phage display method for specificity against ESAT-6. The high affinity “clones” are selected and scaled for ESAT-6 specific DARPin.

2.2. Detection principle and signal flow

The detection of specific TB antigen (ESAT-6) is performed as follows:

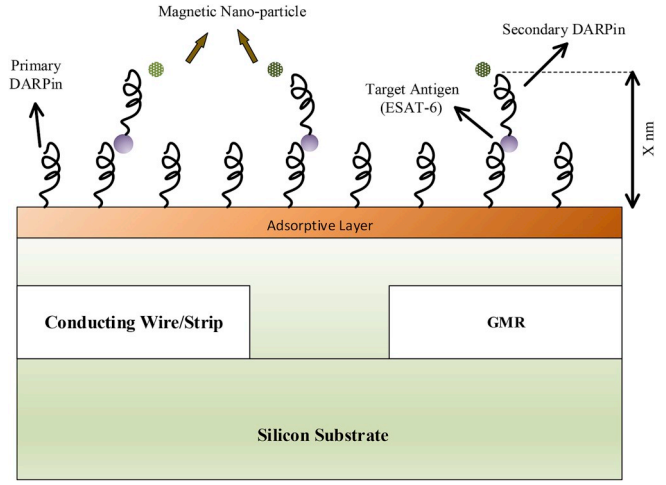

Fig. 2. Schematic Representation of DARPin Based GMR biosensor.

1. A current is passed through conducting wire and the resistance of (or current through) the GMR is measured.
2. As shown in Fig. 2, primary DARPins specific to ESAT-6 work as capture antibody as in case of sandwich ELISA. The biosensor is first exposed to the blood sample containing the MTB specific ESAT-6 and the antigens compatible to the antibodies in the immobilized DARPins attach to the surface.
3. The Biosensor is then exposed to other liquid containing the ESAT-6 specific secondary DARPin. These DARPins are bounded with nano-magnetic particles (beads) for the purpose of labeling as shown in Fig. 2. In Fig. 2, x nm represents the total height of sandwich product of primary DARPin, antigen and secondary DARPin.
4. The presence of magnetic nano-particles affects the magnetic field produced by the conducting wire and the density of beads is proportional to the ESAT-6 concentration. So, the ESAT-6 concentration is measured by measuring the change in resistance (with respect to step 1) of GMR. Fig. 3 represents the overall working principle of GMR biosensor for the early stage TB detection.

3. Mathematical modelling

The DARPin-antigen reaction in the proposed GMR biosensor forms a sandwich immunoassay. Firstly, the ESAT-6 specific DARPin referred to as primary DARPin is immobilized to a reference surface and then the sample containing the target is added. The reaction takes place and is allowed to reach at equilibrium. After this, a secondary ESAT-6 specific secondary DARPin labeled with a magnetic nanoparticle is added forming a sandwich platform. Finally, the amount of bounded label is measured by applying an external magnetic field. The signal generated is proportional to the final product concentration. The whole process can be described by Fig. 2 and can be represented symbolically by the following equations [19]:

$$\begin{aligned} A + B_1 &\rightleftharpoons C_1 \\ D + B_1 &\rightleftharpoons C_2 \\ A + B_2 &\rightleftharpoons D \\ C_1 + B_2 &\rightleftharpoons C_2 \end{aligned} \quad (1)$$

where.

A represents antigen ESAT-6,
B_1 represents immobilized primary DARPin,
B_2 represents magnetic nanoparticles labeled secondary DARPin,
C1 represents the product of A (ESAT-6) and B1 (primary DARPin),
D represents the product of A (ESAT-6) and B_2 (secondary DARPin), and
C_2 represents the final sandwich product of C_1 and B_2

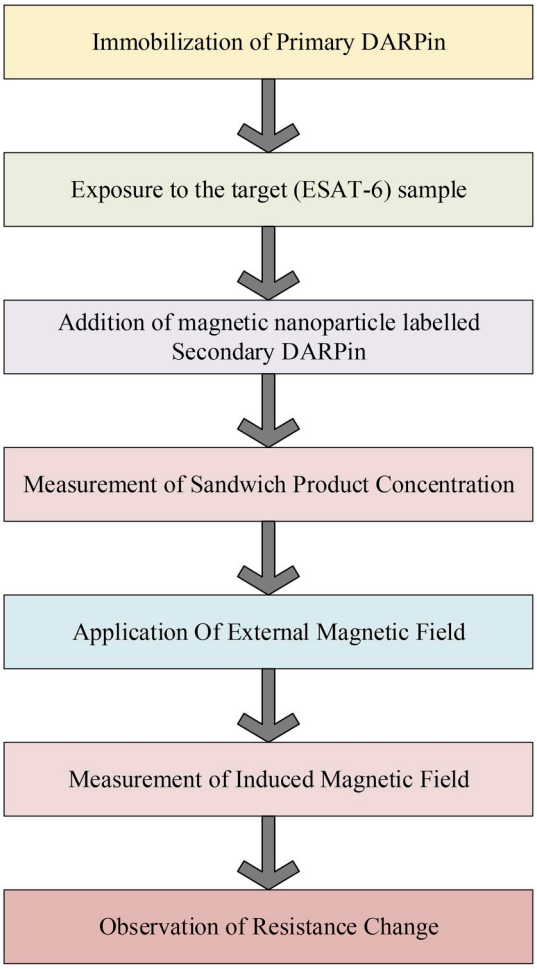

Fig. 3. Working principle of GMR biosensor.

'k_1' is the forward reaction rate and 'k_{-1}' is the reverse reaction rate of first two reactions whereas and 'k_2' and 'k_{-2}' are the forward and reverse reaction rates of third and fourth reactions.

The concentrations of different reactants and products (denoted by square brackets) are represented by their corresponding lower case letters as shown below:

$$a = [A],\ b_1 = [B_1],\ b_2 = [B_2],\ c_1 = [C_1],\ d = [D],\ c_2 = [C_2] \quad (2)$$

For the mathematical modeling, the initial conditions are symbolized as:

$$a(0) = \alpha,\ b_1(0) = \beta_1,\ b_2(0) = \beta_2,\ c_1(0) = 0,\ d(0) = 0,\ c_2(0) = 0 \quad (3)$$

Here, α, β_1 and β_2 are constants. For the experimental requirements, α should be less than β_1 and β_2 (i.e. $\alpha < \beta_1$ and $\alpha < \beta_2$).

For the simplified calculations, system should be non-dimensional. In order to non-dimensionalize the system, all the concentrations of eq. (2) and eq. (3) are divided by β1 and modified concentrations are represented as:

$$a = a/\beta_1,\ b_1 = b_1/\beta_1,\ b_2 = b_2/\beta_1,\ c_1 = c_1/\beta_1,\ d = d/\beta_1,\ c_2 = c_2/\beta_1 \quad (4)$$

$$a(0) = a/\beta_1,\ b_1(0) = 1,\ b_2(0) = \beta_2/\beta_1,\ c_1(0) = 0,\ d(0) = 0,\ c_2(0) = 0 \quad (5)$$

Following set of non-linear differential equations (representing the steady-state forms) can describe the kinetic behavior of each reactant involved in the reactions shown in eq. (1). A +

$$da/dt = K_{-1}\, c_1 + K_{-2}\, d - a\, b_1 - K^1\, a\, b_2$$

$$db_1/dt = K_{-1}(c_1 + c_2) - b_1(a + d)$$

$$db_2/dt = K_{-2}(c_2 + d) - K^1 b_2(a + c_1)$$

$$dc_1/dt = a\,b_1 - K_{-1}c_1 - K^1 b_2 c_1 + K_{-2}c_2$$

$$dd/dt = K^1 a\,b_2 - K_{-2}\,d - b_1\,d + K_{-1}\,c_2$$

$$dc_2/dt = K^1 b_2 c_1 + b_1 d - (K_{-1} + K_{-2})\,c_2 \quad (6)$$

where,

$$K_{-1} = k_{-1}/(\beta_1 k_1),\ K_{-2} = k_{-2}/(\beta_1 k_1),\ K^1 = k_2/k_1 \quad (7)$$

The conservation laws followed are:

$$a + c_1 + c_2 + d = \alpha/\beta_1$$

$$b_1 + c_1 + c_2 = 1$$

$$b_2 + c_2 + d = \beta_2/\beta_1 \quad (8)$$

From equations (6) and (8), we can find that:

$$b_1^2 + (\alpha/\beta_1 - 1 + K_{-1})\,b_1 - K_{-1} = 0,$$

$$b_2^2 + ((\alpha-\beta_2)/\beta_1 + K_{-2}/K^1)\,b_2 - (K_{-2}\,\beta_2)/(K^1\beta_1) = 0, \quad (9)$$

$$c_2 = \frac{\frac{\beta_2}{\beta_1} b_1 + K'\beta_2 - (1 + K')\,b_1\,b_2}{b_1 + K_{-1} + K'\beta_2} \quad (10)$$

equation (10) gives the total concentration of sandwich product which will enable the measurement of target antigen (ESAT-6 in our case). As external magnetic field is applied, bounded magnetic nanoparticles (proportional to the concentration c2) induce magnetic field which will change the overall resistance of GMR biosensor. If the external magnetic field is applied in z-direction, then the induced magnetic field will be in x-direction. Since the GMR biosensor can detect only in x-direction, so the x-component of magnetic field (induced magnetic field) is detected without any interference from z-component (external magnetic field) [6]. The magnetic field induced in x-direction by a single nanoparticle on the application of external magnetic field in z-direction is given as [20]:

$$B_X = \mu_0\, M\, \frac{a^3(a + t + x)\,d}{[(a + t + x)^2 + d^2]^{5/2}} \quad (11)$$

where.

M = external magnetic field in z-direction
a = radius of magnetic nanoparticle
t = thickness of top adsorptive layer
x = total height of sandwich product of primary DARPin, antigen and secondary DARPin as shown in Fig. 2
d = distance of induced magnetic field B_x along the trace and relative to the center of the magnetic nanoparticle as shown in Fig. 4.

This induced magnetic field will have a maximum value when d = (a + (t + x))/2 [20]. For the detection of TB, we have assumed the adsorptive layer with the thickness of t = 0.35 nm. Since the average height of antibody-antigen product is around 6.6 ± 0.3 nm [21], so the total average height of sandwich product of primary DARPin, antigen and secondary DARPin is assumed to be around x ≈ 10 nm. With the application of varied magnetic field and use of different sized nanoparticles, the strength of induced magnetic field can be altered. The total induced magnetic field can then be obtained by multiplying the total sandwich product concentration (c_2) and the magnetic field induced by a single nanoparticle (B_x) with an assumption that magnetic field induced by each nanoparticle will not influence other induced magnetic fields. This total induced magnetic field component contributes to a change in overall sensor resistance.

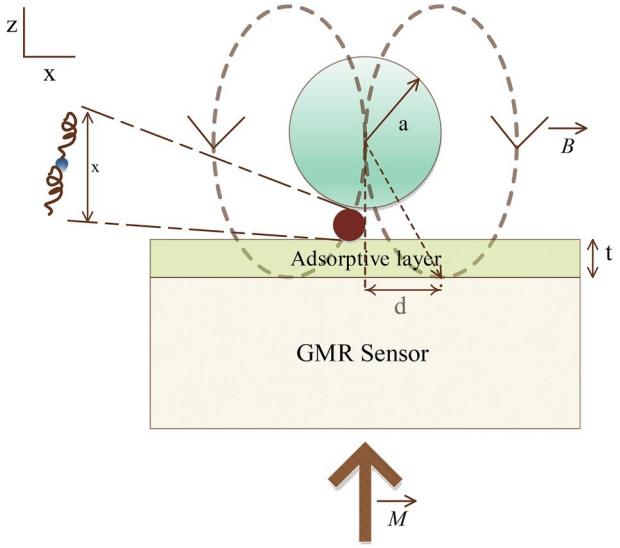

Fig. 4. Detection of induced magnetic field by a magnetic nanoparticle on GMR structure.

4. Results and discussion

TB is a contagious deadly infection that can easily spread. In this study, we focused on developing a highly specific, sensitive and portable platform for TB diagnostics at initial stages. Since, ESAT-6 is one of the preeminent proteins that are secreted early by M. Tuberculosis, thus it is an appropriate candidate for TB detection at early phases [22]. Recently, Lakshmipriya et al. [23] have detected ESAT-6 by gold nanoparticle (GNP) assisted ELISA method and have compared the results with the conventional ELISA technique. In order to detect the low amounts of ESAT-6 from MTB, we incorporated DARPins in sandwich assay instead of ESAT-6 specific antibodies and then detected the presence of target using GMR biosensing platform. In the following section, the results from conventional ELISA, GNP-assisted ELISA and DARPin based GMR strategies have been compared.

4.1. Conventional ELISA

ELISA (Enzyme-linked immunosorbent assay) technique has been extensively used to screen the several diseases by detecting antigenic proteins using an appropriate antibody [18,24–26]. In comparison to the other standard techniques, ELISA have shown better performance in terms of cost, easy operability, high sensitivity, and no use of hazardous materials [27–30]. ESAT-6 detection by conventional ELISA, with the concentrations of capture antibody and labeled secondary antibody as 100 and 0.1 μg/mL (β_1 and b_1) and 10 and 0.2 mg/mL (β_2 and b_2) respectively (as demonstrated by Lakshmipriya et al. [23]), has the limit of detection of up to 30 nM with the optical density (OD) of 0.08.

4.2. GNP assisted ELISA

The current research focus is on the use of gold nanoparticles (GNPs) in biosensor development due to their excellent stability and sensitivity [31]. In biosensors, gold has proven to be an ideal substrate choice for immobilizing aptamers [32], antibodies [33,34], antigen, and other biomolecules [23,24]. Lakshmipriya et al. [23] have described the GNP-assisted ELISA technique for early stage diagnosis of TB by targeting ESAT-6. It has been shown that incorporation of GNPs into ELISA resulted in an improved ESAT-6 detection by 7.5 folds than conventional ELISA strategy. Fig. 5 shows the performance comparison of conventional and GNP-assisted ELISA employing 10 nm GNPs. Further, the size of GNPs also affected the sensitivity. Large-sized GNPs

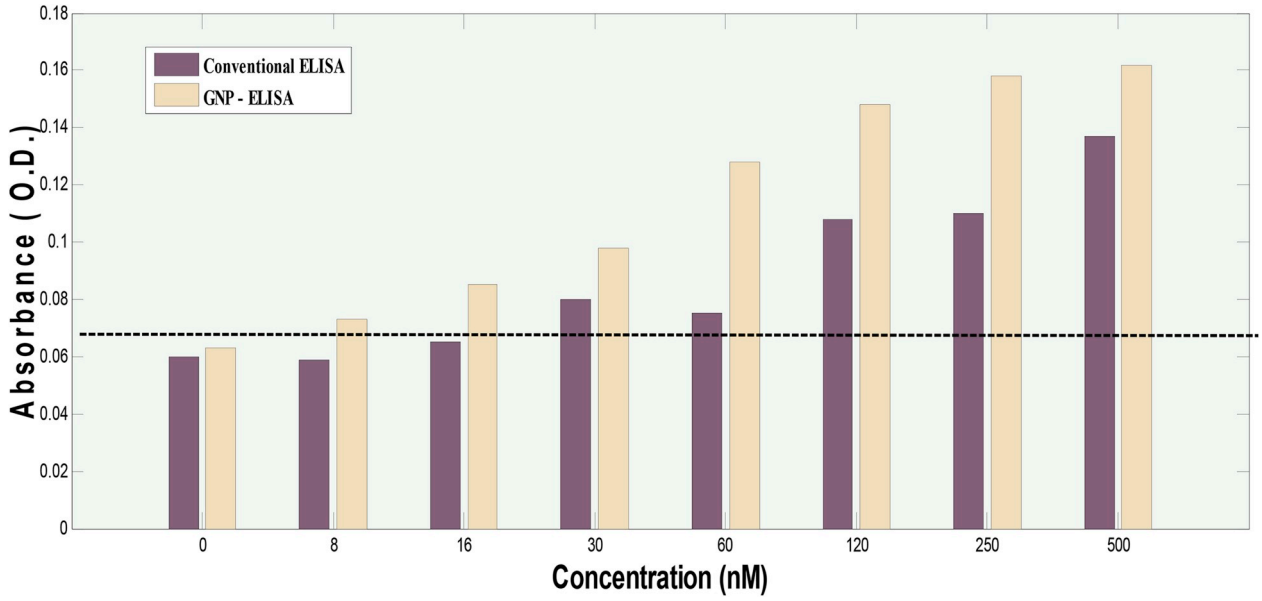

Fig. 5. Performance Comparsion of conventional ELISA Vs 10 nm GNP- assisted ELISA.

(80 nm) reported a higher sensitivity (or lower limit of detection) of 4 nM than 8 nM achieved by smaller sized GNP (10 nm) [23].

4.3. GMR technique

Compared with the widely used traditional optical detection (as used in ELISA) techniques in biomedicine, GMR biosensors are portable, more sensitive, and give a fully electronic readout [35,36]. In addition, the magnetic nanoparticles used in GMR do not bleach unlike fluorescent labels employed in immunofluorescence techniques like ELISA [37]. The presence of specific proteins in complex body fluids like saliva, urine or blood provides very specific information about the health of an individual. Detection and measurement of these proteins is difficult to the low concentration (5–50 ng/mL) and in limited sample volumes. With the proposed GMR technique by applying 50 Oe (Oersted) of external magnetic field and employing magnetic nanoparticle of 40 nm radius, it is possible to achieve the limit of detection for ESAT-6 in the range of pg/ml (1 pg/mL = 0.167 pM) as shown in Fig. 6, thus resulting in a highly sensitive TB detection than GNP-assisted ELISA technique. The simulated results are in accordance with the mathematical calculations and the performance analysis is shown in Fig. 6. Fig. 6A shows that the averaged signal strength for 1 pM of ESAT-6 is 0.72 μT and it goes up with the ESAT-6 concentration and reaches to 359 mT for 500 nM ESAT-6.

Depending upon the structural composition of magnetic nanoparticles, the signal strength can be increased by applying higher external magnetic fields. For instance, for NiFe magnetic nanobeads, external magnetic field in the range of 29 kA/m can be applied [20] and it results in the enhanced signal strength of 5.23 μT for 1 pM concentration of ESAT-6 leading to the higher sensitivity and lower limit of detection. The size of magnetic nanoparticles also affects the sensitivity of GMR biosensor. Large-sized nanoparticles (40 nm radius or 80 nm MNP) have higher signal strengths for low concentrations than small sized (5 nm radius or 10 nm MNP). For magnetic nanoparticle of 5 nm radius, the signal strength for 1 pM ESAT-6 concentration is 50 nT whereas for 40 nm radius, the signal strength improves to 0.72 μT (~14 fold higher). Fig. 6B shows the influence of different sized magnetic nanoparticles on the overall performance of GMR biosensor. Table 1 compares the overall performance, in terms of limit of detection; signal strength and particle size, of conventional ELISA, GNP-ELISA and GMR techniques for TB diagnostic application.

Further, magnetic markers have numerous advantages, the prominent one being the fact that in the sample solution, all other components are essentially non-magnetic and also the biological samples are deprived of ferromagnetism properties [38], thus jettisoning interference effects and reducing the background signal, eventually leading to the specific target detection. In our technique, we have employed ESAT-6 compatible DARPins which are much more specific in detecting the target and are 10 times less in size (around 14–18 kDa) than antibodies [39]. Moreover, DARPins have better thermal and thermodynamic stability and are also stable in human blood serum [40–42]. These ESAT-6 specific DARPins have high potency making them active at even low concentrations [43] and with the increase in the concentration of ESAT-6, more magnetic nanoparticles labeled DARPins target the antigen leading to the enhance detection by GMR sensor. The proposed DARPins based GMR biosensor gives the results in less time than ELISA due to the fact that the magnetic actuation of nanobeads/nanoparticles is fast as compared to slow diffusion in other detection methods.

5. Conclusion

GMR technique employing DARPins and magnetic nanoparticles can be of immense use in eradicating the TB and achieving the technological breakthroughs as per End TB strategy. Based on the erstwhile discussion, it can be concluded that the proposed methodology has enormous features and is suitable for the point-of-care detection of TB with high specificity by targeting the early secreted *MTB* specific protein ESAT-6. In comparison with the existing TB detection techniques, the limit of detection attained with this biosensing technique is in the range of pg/mL to few ng/mL resulting in the higher sensitivity. The sensitivity can further be improved by altering the structural composition and size of magnetic nanoparticles. Further, due to the possibility of real integration of GMR sensors with many other standard technologies, this technique can be extended for the detection of other malignant pathogens (like HIV) and drug-resistant mutants.

Acknowledgment

We are grateful to Dr. Purva Bhatter (Post Doc., IIT Madras) for her constant help and technical guidance.

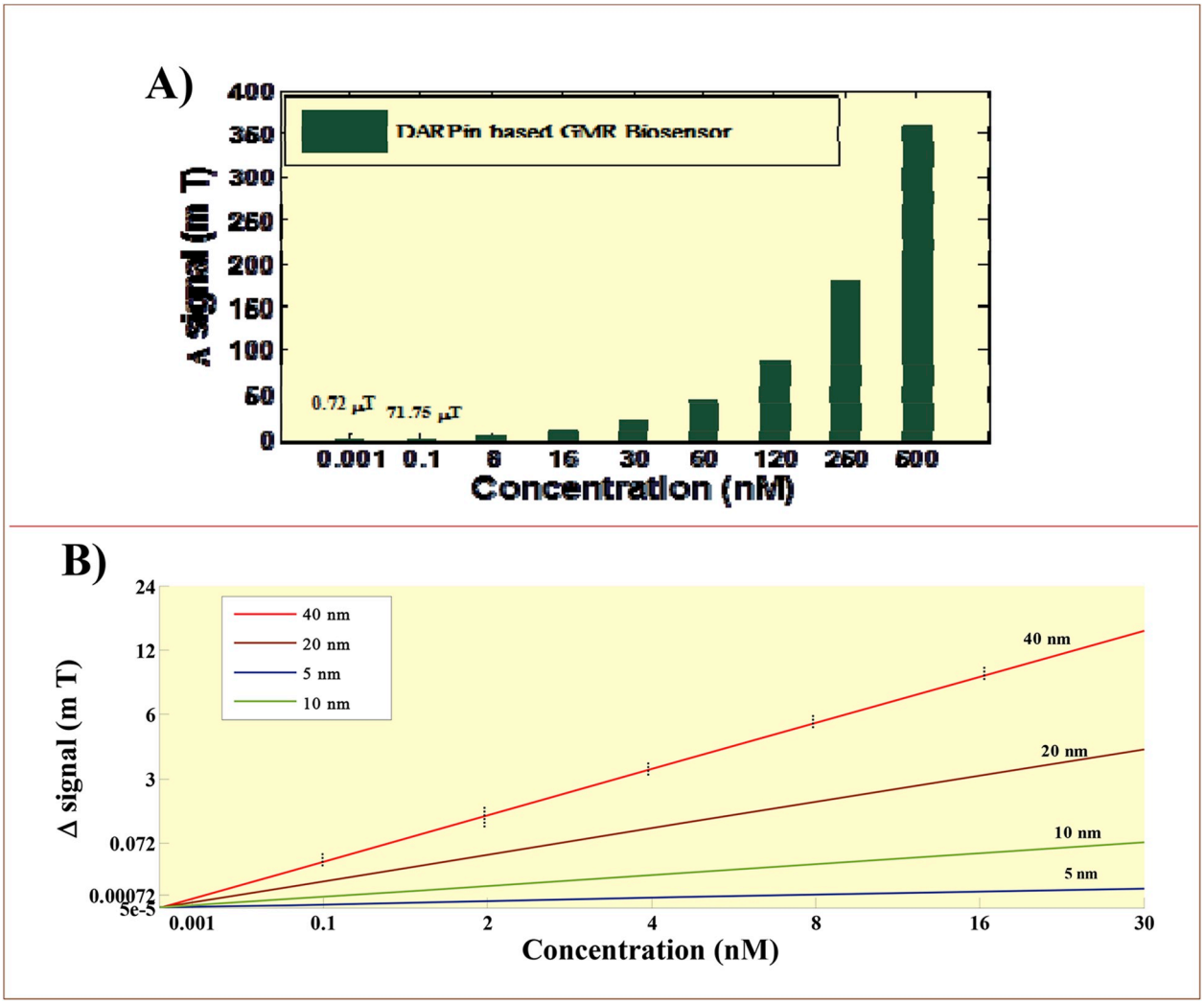

Fig. 6. Performance Analysis of DARPin based GMR biosensor. A) Signal Strength Vs ESAT-6 Concentration. B) Effetct of magnetic nanoparticles having different radius size on signal strengths.

Table 1
Performance Comparison of Conventional ELISA, GNP-ELISA and GMR for TB specific ESAT-6 detection.

TECHNIQUE	LIMIT OF DETECTION	SIGNAL STRENGTH	PARTICLE SIZE
Conventional ELISA	30 nM	0.08 O.D	–
GNP-ELISA	8 nM	0.099 O.D	10 nm
	4 nM	0.132 O.D	80 nm
GMR	1 pM	50 nT	10 nm
		0.17 μT	20 nm
		0.41 μT	40 nm
		0.72 μT	80 nm

Appendix A. Supplementary data

Supplementary data to this article can be found online at https://doi.org/10.1016/j.tube.2019.07.003.

References

[1] WorldHealthOrganization. Global tuberculosis report. 2017978-92-4-156551-6. 2017 https://apps.who.int/iris/handle/10665/259366. License: CC BY-NC-SA 3.0 IGO.
[2] Gupta S, Kakkar V. Recent technological advancements in tuberculosis diagnostics-A review. Biosensors and Bioelectronics; 2018.
[3] Devkota J, Ruiz A, Mukherjee P, Srikanth H, Phan M-H. Magneto-impedance biosensor with enhanced sensitivity for highly sensitive detection of nanomag-D beads. IEEE Trans Magn 2013;49:4060–3.
[4] Li F, Kosel J. A magnetic biosensor system for detection of E. coli. IEEE Trans Magn 2013;49:3492–5.
[5] Baibich MN, Broto JM, Fert A, Van Dau FN, Petroff F, Etienne P, et al. Giant magnetoresistance of (001) Fe/(001) Cr magnetic superlattices. Phys Rev Lett 1988;61:2472.
[6] Djamal M. Giant magnetoresistance material and its potential for biosensor applications. International conference on instrumentation, communication. vol. 2009. Information Technology, and Biomedical Engineering; 2009. p. 1–6.
[7] Mathon J. Phenomenological theory of giant magnetoresistance. Spin electronics. Springer; 2001. p. 71–88.
[8] Wang Y, Wang W, Yu L, Tu L, Feng Y, Klein T, et al. Giant magnetoresistive-based biosensing probe station system for multiplex protein assays. Biosens Bioelectron 2015;70:61–8.
[9] Cubells-Beltrán M-D, Reig C, Madrenas J, De Marcellis A, Santos J, Cardoso S, et al. Integration of GMR sensors with different technologies. Sensors 2016;16:939.
[10] Zhang Y, Zhou D. Magnetic particle-based ultrasensitive biosensors for diagnostics. Expert Rev Mol Diagn 2012;12:565–71.
[11] Team GGMB. Magnetic biosensing [Online]. Available:. http://www.nanospin.umn.edu/magnetic-biosensing.
[12] Wang W, Wang Y, Tu L, Klein T, Feng Y, Li Q, et al. Magnetic detection of mercuric ion using giant magnetoresistance-based biosensing system. Anal Chem 2014;86:3712–6.
[13] Krishna VD, Wu K, Perez AM, Wang J-P. Giant magnetoresistance-based biosensor for detection of influenza A virus. Front Microbiol 2016;7:400.
[14] Wu K, Klein T, Krishna VD, Su D, Perez AM, Wang J-P. Portable GMR handheld platform for the detection of influenza A virus. ACS Sens 2017;2:1594–601.
[15] Chen Y-T, Kolhatkar AG, Zenasni O, Xu S, Lee TR. Biosensing using magnetic particle detection techniques. Sensors 2017;17:2300.

[16] Pandey H, Fatma F, Yabaji SM, Kumari M, Tripathi S, Srivastava K, et al. Biophysical and immunological characterization of the ESX-4 system ESAT-6 family proteins Rv3444c and Rv3445c from Mycobacterium tuberculosis H37Rv. Tuberculosis 2018;109:85–96.
[17] Brock I, Munk M, Kok-Jensen A, Andersen P. Performance of whole blood IFN-γ test for tuberculosis diagnosis based on PPD or the specific antigens ESAT-6 and CFP-10. Int J Tuberc Lung Dis 2001;5:462–7.
[18] Geluk A, van Meijgaarden KE, Franken KL, Subronto YW, Wieles B, Arend SM, et al. Identification and characterization of the ESAT-6 homologue of Mycobacterium leprae and T-cell cross-reactivity with Mycobacterium tuberculosis. Infect Immun 2002;70:2544–8.
[19] Wang Q. Mathematical methods for biosensor models. 2011.
[20] Rife J, Miller M, Sheehan P, Tamanaha C, Tondra M, Whitman L. Design and performance of GMR sensors for the detection of magnetic microbeads in biosensors. Sens Actuators A Phys 2003;107:209–18.
[21] Ierardi V, Ferrera F, Millo E, Damonte G, Filaci G, Valbusa U. Bioactive surfaces for antibody-antigen complex detection by Atomic Force Microscopy. Journal of physics. Conference Series; 2013:012001.
[22] Wang X, Barnes PF, Dobos-Elder KM, Townsend JC, Chung Y-t, Shams H, et al. ESAT-6 inhibits production of IFN-γ by Mycobacterium tuberculosis-responsive human T cells. J Immunol 2009;182:3668–77.
[23] Lakshmipriya T, CB Gopinath S, Citartan M, Hashim U, Tang T-H. Gold nanoparticle-mediated high-performance enzyme-linked immunosorbent assay for detection of tuberculosis ESAT-6 protein. Micro Nanosyst 2016;8:92–8.
[24] Gopinath SC, Anbu P, Lakshmipriya T, Tang T-H, Chen Y, Hashim U, et al. Biotechnological aspects and perspective of microbial keratinase production. BioMed Res Int 2015;2015.
[25] Gopinath SC, Awazu K, Fujimaki M, Shimizu K. Evaluation of anti-A/Udorn/307/1972 antibody specificity to influenza A/H3N2 viruses using an evanescent-field coupled waveguide-mode sensor. PLoS One 2013;8:e81396.
[26] Toh SY, Citartan M, Gopinath SC, Tang T-H. Aptamers as a replacement for antibodies in enzyme-linked immunosorbent assay. Biosens Bioelectron 2015;64:392–403.
[27] Poongodi GL, Suresh N, Gopinath SC, Chang T, Inoue S, Inoue Y. Dynamic change of neural cell adhesion molecule polysialylation on human neuroblastoma (IMR-32) and rat pheochromocytoma (PC-12) cells during growth and differentiation. J Biol Chem 2002;277:28200–11.
[28] Liu Q-L, Yan X-H, Yin X-M, Situ B, Zhou H-K, Lin L, et al. Electrochemical enzyme-linked immunosorbent assay (ELISA) for α-fetoprotein based on glucose detection with multienzyme-nanoparticle amplification. Molecules 2013;18:12675–86.
[29] Li X, Li G, Teng Q, Yu L, Wu X, Li Z. Development of a blocking ELISA for detection of serum neutralizing antibodies against newly emerged duck Tembusu virus. PLoS One 2012;7:e53026.
[30] Guimaraes AJ, Pizzini CV, de Matos Guedes HL, Albuquerque PC, Peralta JM, Hamilton AJ, et al. ELISA for early diagnosis of histoplasmosis. J Med Microbiol 2004;53:509–14.
[31] Saha K, Agasti SS, Kim C, Li X, Rotello VM. Gold nanoparticles in chemical and biological sensing. Chem Rev 2012;112:2739–79.
[32] Gopinath SC, Lakshmipriya T, Awazu K. Colorimetric detection of controlled assembly and disassembly of aptamers on unmodified gold nanoparticles. Biosens Bioelectron 2014;51:115–23.
[33] Gopinath SC, Awazu K, Fujimaki M, Shimizu K, Shima T. Observations of immunogold conjugates on influenza viruses using waveguide-mode sensors. PLoS One 2013;8:e69121.
[34] Kim S, Lee J, Lee SJ, Lee HJ. Ultra-sensitive detection of IgE using biofunctionalized nanoparticle-enhanced SPR. Talanta 2010;81:1755–9.
[35] Zhi X, Deng M, Yang H, Gao G, Wang K, Fu H, et al. A novel HBV genotypes detecting system combined with microfluidic chip, loop-mediated isothermal amplification and GMR sensors. Biosens Bioelectron 2014;54:372–7.
[36] Sun X, Zhi S, Lei C, Zhou Y. Investigation of contactless detection using a giant magnetoresistance sensor for detecting prostate specific antigen. Biomed Microdevices 2016;18:60.
[37] Eickenberg B, Meyer J, Helmich L, Kappe D, Auge A, Weddemann A, et al. Lab-on-a-chip magneto-immunoassays: how to ensure contact between superparamagnetic beads and the sensor surface. Biosensors 2013;3:327–40.
[38] Zhang X, Reeves DB, Perreard IM, Kett WC, Griswold KE, Gimi B, et al. Molecular sensing with magnetic nanoparticles using magnetic spectroscopy of nanoparticle Brownian motion. Biosens Bioelectron 2013;50:441–6.
[39] Plückthun A. Designed ankyrin repeat proteins (DARPins): binding proteins for research, diagnostics, and therapy. Annu Rev Pharmacol Toxicol 2015;55:489–511.
[40] Binz HK, Stumpp MT, Forrer P, Amstutz P, Plückthun A. Designing repeat proteins: well-expressed, soluble and stable proteins from combinatorial libraries of consensus ankyrin repeat proteins. J. Molecular Biol. 2003;332:489–503.
[41] Kohl A, Binz HK, Forrer P, Stumpp MT, Plückthun A, Grütter MG. Designed to be stable: crystal structure of a consensus ankyrin repeat protein. Proc Natl Acad Sci 2003;100:1700–5.
[42] Wetzel SK, Settanni G, Kenig M, Binz HK, Plückthun A. Folding and unfolding mechanism of highly stable full-consensus ankyrin repeat proteins. J. Molecular Biol. 2008;376:241–57.
[43] Zahnd C, Kawe M, Stumpp MT, de Pasquale C, Tamaskovic R, Nagy-Davidescu G, et al. Efficient tumor targeting with high-affinity designed ankyrin repeat proteins: effects of affinity and molecular size. Cancer Res 2010;70:1595–605.